11th Australasian Fluid Mechanics Conference
University of Tasmania, Hobart, Australia
14-18 December 1992

VISCOUS-INVISCID COUPLING IN SHIP HYDRODYNAMICS

E. CAMPANA, A. DI MASCIO, P.G. ESPOSITO and F. LALLI

INSEAN, Italian Ship Model Basin
Via di Vallerano 139, 00128 Roma, ITALY

INTRODUCTION

The solution of free surface viscous flows is one of the most important topics in naval architecture. The numerical simulation of this flow field is very difficult, because of the extremely large Reynolds numbers in practical problems ($\sim 10^8 \div 10^9$), and the additional complication due to the moving boundary at the air–water interface. The solution of the Navier–Stokes equations in the whole domain requires a large amount of computer memory and CPU time, while the inviscid model (although much cheaper in terms of computer resources) is unable to mimic the formation and growth of boundary layer and wake.

In the analysis of this kind of flows, the zonal approach concepts can be fruitfully exploited to save both computer storage and CPU time. The full viscous model is solved only in the neighbourhood of rigid boundaries and wakes, while the external flow, where viscous effects are supposed to be negligible, is simulated by a linearized inviscid model (Dawson, 1977) whose capability of representing the free surface dynamics is generally satisfactory (Lalli et al, 1992). The choice of the linear model has been made in view of the extention of the zonal approach to the analysis of three–dimensional flows past ship hulls, for which a full nonlinear solution would be too expensive.

However, when using zonal approach, problems related to the matching conditions for the external and the internal solutions arise. Although the coupling procedure in unbounded flows is quite well established (see, e.g. Lock and Williams, 1987), the use of a linearized potential solver for external free surface flow gives rise to new difficulties.

In the following sections, the viscous and inviscid solvers are briefly described. Then, the aforementioned problems in the coupling are analyzed and a possible way to face them is proposed. Finally some numerical examples are discussed and compared with experimental data (Salvesen 1966).

THE INVISCID PROBLEM

The calculation of the free surface flow past submerged or floating bodies with forward speed is usually performed with potential solvers, being the wave propagation mainly determined by inertial and pressure forces. Let us consider the irrotational two–dimensional steady flow in the domain D, bounded by the water–air interface S and by the curve Γ (closed or not) on which Neumann boundary conditions are forced (see fig.1). The variables are

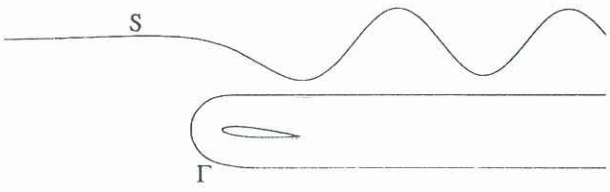

Figure 1: Computational domain

nondimensionalized with respect to the free stream velocity U and a characteristic length L (e.g. body chord). We assume that the flow velocity $\vec{u} = (u, v)$ can be written as $\vec{u} = \nabla\phi$. The potential ϕ satisfies Laplace equation inside the flow field:

$$\nabla^2\phi = 0 \tag{1}$$

The boundary condition on Γ is

$$\phi_n = \psi \tag{2}$$

being ψ assigned ($\psi = 0$ at rigid boundaries at rest). The shape of the free boundary S is unknown, being related to the solution by the dynamic condition:

$$y = \eta(x) = \frac{Fr^2}{2}(1 - \nabla\phi \cdot \nabla\phi) \tag{3}$$

On this surface, the solution ϕ satisfies

$$\frac{Fr^2}{2}\nabla\phi \cdot \nabla(\nabla\phi \cdot \nabla\phi) + \phi_z = 0. \tag{4}$$

Finally a condition at infinity must be imposed:

$$\lim_{x \to -\infty} |\nabla \phi| = 1 \tag{5}$$

The nonlinear inviscid problem is linearized following the procedure suggested by Dawson (1977). The velocity potential ϕ is split into two terms:

$$\phi(x,y) = \varphi(x,y) + \tilde{\varphi}(x,y) \tag{6}$$

In (6) the term $\varphi(x,y)$ is the double model potential (i.e. the potential due to Γ and its image with respect to $y = 0$), while the free surface potential $\tilde{\varphi}(x,y)$ takes into account the interaction between Γ and S. The solution is expressed in terms of a simple layer:

$$\varphi(x,y) = \int_\Gamma \sigma \, \log(r \cdot r') \, d\gamma \tag{7}$$

$$\tilde{\varphi}(x,y) = \int_\Gamma \tilde{\sigma} \, \log r \, d\gamma + \int_S \tilde{\sigma} \, \log r \, ds \tag{8}$$

where σ is the source density while r (r') is the distance of the field point from the source point (image source point). The boundaries Γ and S are discretized with flat elements while the density is approximated with a piecewise constant function.

The double model potential is solved with the boundary condition

$$\varphi_n = \psi \tag{9}$$

and is characterized by the property $\varphi_y(x,0) = 0$. This solution gives the zero-Froude number flow which is used as basis flow for the linearization.

The free surface flow is solved using the linearized boundary condition

$$\varphi_x^2 \tilde{\varphi}_{xx} + 2\varphi_x \varphi_{xx} \tilde{\varphi}_x + \frac{\tilde{\varphi}_y}{Fr^2} = -\varphi_x^2 \varphi_{xx} \qquad \text{on } y = 0 \tag{10}$$

while

$$\tilde{\varphi}_n = 0 \qquad \text{on } \Gamma \tag{11}$$

Next the new free surface comes from the linearized form of eq. (3):

$$y = \frac{Fr^2}{2}(1 - \varphi_x^2 - 2\varphi_x \tilde{\varphi}_x) \tag{12}$$

THE VISCOUS PROBLEM

Viscous effects are dominant in the region close to the body and in the wake, where separation of boundary layer and formation of vortices occur. The solution of the Navier-Stokes equations is required in these regions.

For steady problems, the governing equations of the viscous flow are

$$\frac{\partial}{\partial x_j}(u_j u_i) + \frac{\partial p}{\partial x} = \frac{\partial}{\partial x_j}(\tau_{ij}) \tag{13}$$

$$\frac{\partial u_j}{\partial x_j} = 0 \tag{14}$$

where the index notation has been adopted, $p = P/\rho$ and τ_{ij} is the viscous stress

$$\tau_{ij} = (\nu + \nu_T)\left(\frac{\partial u_i}{\partial x_j} + \frac{\partial u_j}{\partial x_i}\right) \tag{15}$$

ν_T is the turbulent viscosity, defined by the Baldwin and Lomax (1978) algebraic model.

The Reynolds Averaged Navier-Stokes equations (13-14) are discretized using a finite volume scheme and are integrated in time using a pseudo-compressibility implicit scheme developed by Kwak et al. (1986). In this scheme, pressure and Cartesian components of velocity are located at the center of the cell. The flux at cell interfaces are computed by simple averaging and centered differencing. A numerical high-order dissipation is introduced to stabilize the calculation, while a local time step is used to speed up the convergence rate. Approximate factorization technique is used to split the coefficient matrix into two block tridiagonal matrices, for which an efficient solution algorithm exists.

THE COUPLED PROBLEM

One of the crucial points in viscous–inviscid coupling is the position of the surface at which the matching must be imposed. Several possibilities have been explored in aerodynamics: at the outer edge of the shear layers, on the displacement surface, on the body surface using the transpiration velocity concept (Lock and Williams,1987). In this paper an approach similar to that suggested by Dinh et al. (1987) has been used, but no overlapping region is introduced to match inner and outer solution. The location of the surface Γ is decided *a priori* and kept fixed during the computation. Its distance from the solid body is such that viscous effects are assumed to be negligible outside it. The obvious advantage of this strategy is that regridding is needed neither for the outer nor for the inner solver.

When dealing with aerodynamics problems, the matching of the two solutions is iteratively obtained using:

i) the normal velocity computed at $A \in \Gamma$ (see fig. 2) with the viscous solver as boundary value for the normal derivative of the potential

$$\varphi_n = \psi = \vec{u^v} \cdot \vec{n} \qquad \text{on } \Gamma \tag{16}$$

ii) the pressure and the tangential velocity computed at $A \in \Gamma$ with the potential solver as boundary values for the Navier-Stokes equations.

Additional problems arise from the presence of a moving interface in the fluid domain: in fact, although the potential free surface solver is linearized (Dawson, 1977), the approach described before gives unsatisfactory results, regarding both wave height and length. Therefore, the coupling procedure has been split into two separate stages.

Stage 1: The Basis Flow

In the first one, the basis flow around Γ and its image is computed by means of an iterative procedure consisting of the following steps:

(a) From the previous viscous step we solve the external flow using the following boundary condition on Γ:

$$\varphi_n = \vec{u}^v \cdot \vec{n} \qquad (17)$$

where $\vec{u}^v \cdot \vec{n}$ is the normal component of the viscous velocity at Γ (see fig. 2).

(b) The values of tangential component of potential velocity $\vec{u}^p \cdot \vec{t}$ and pressure at Γ are then used as boundary conditions for the viscous problem.

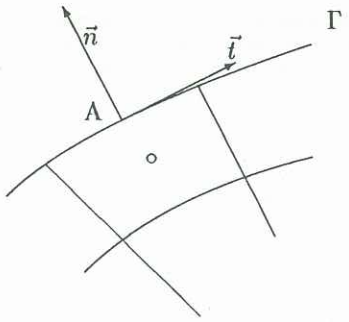

Figure 2: Matching surface Γ and variable collocation

At each global iteration the viscous solution is carried on until the L_2 residual on divergence R^{k+1} becomes smaller than αR^k, where α is assigned (tipically $O(10^{-1})$).

For the convergence of the iterative procedure an underrelaxation factor of 0.2 is used to update the density source σ.

Stage 2: The Free Surface Flow

Once the solution of the basis flow is obtained, the influence of the free surface is taken into account. The boundary conditions for the external flow are:

$$\tilde{\varphi}_n = \vec{u}^v \cdot \vec{n} - \vec{u}^0 \cdot \vec{n} \qquad \text{on } \Gamma \qquad (18)$$

$$\varphi_x^2 \tilde{\varphi}_{xx} + 2\varphi_x \varphi_{xx} \tilde{\varphi}_x + \frac{\tilde{\varphi}_y}{Fr^2} = -\varphi_x^2 \varphi_{xx} \qquad \text{on } y = 0 \quad (19)$$

where $\vec{u}^v \cdot \vec{n}$ is known from the previous viscous computation and $\vec{u}^0$ is the converged double model velocity. Next the free surface is computed from (12).

The iterative procedure is identical to that used in the double model solution. The convergence of the iterative procedure becomes slower and an underrelaxation factor of 0.1, 0.05 is used to update the density source $\tilde{\sigma}$.

NUMERICAL RESULTS

Some sample problems were analyzed to test the reliability of the algorithm. In the first problem no free surface was present. The flow past a NACA 0012 profile at zero incidence and $Re = 10^5$ has been computed using both a large grid with no coupling and a smaller mesh on which the matching procedure has been used (the interface Γ was 0.2 far from the body surface). The computed solutions are compared in terms of pressure contours (fig. 3) and pressure coefficient on the body surface (fig. 4). The convergence of the viscous solution was reached in almost the same number of iterations in both cases. The CPU time decreased linearly with the number of grid points, being the cost of the inviscid computation negligible.

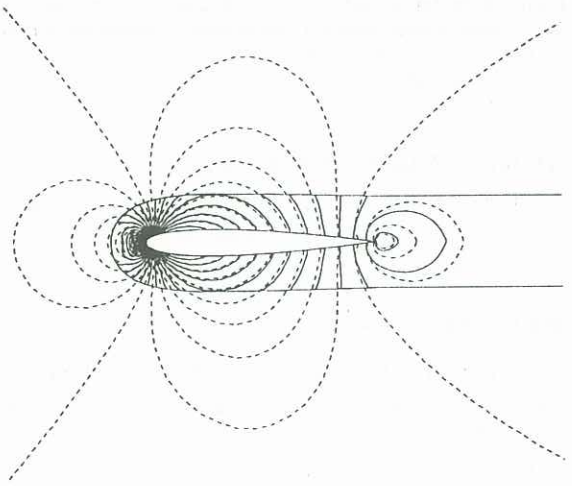

Figure 3: Isolated body: NACA 0012 at zero incidence. $Re = 10^5$. Comparison between the pressure field computed with a 128 x 64 grid without interaction (dashed lines) and the computed field with viscous-inviscid interaction (continuous line) with a 128 x 16 grid. $p_{min} = -0.2$, $p_{max} = 0.42$, $\Delta p = 0.02$

Then free surface effects were analyzed. The inviscid flow around the same NACA 0012 profile, submerged at a depth $h = 1.15$, $Fr = 0.8$, was computed using both the potential solver and the coupled finite volumes-BEM solver. Free surface elevations are shown in fig. 5.

At last, the experiment of Salvesen (1966) was simulated using the proposed algorithm. The numerical free surface elevation is compared with the measured data in fig. 6. The wave length seems to be well predicted by the numerical simulation. The disagreement on the wave amplitude is probably due to the linearization of the potential solver (Lalli et al., 1992), while the differences near the first trough can be attributed to the uncertanties of the turbulence model and the grid resolution in the viscous computation. The convergence history (fig. 7) shows that the discrete equations can be solved within round-off errors.

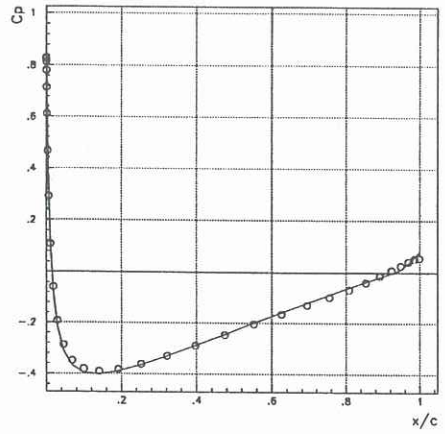

Figure 4: Isolated body: NACA 0012 at zero incidence. $Re = 10^5$. Comparison between the pressure coefficient computed without interaction (solid line) and the C_p computed with viscous–inviscid interaction (o).

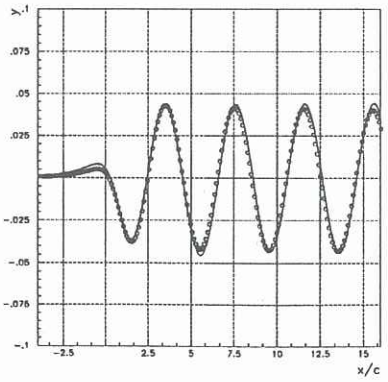

Figure 5: Naca 0012 profile at zero incidence. Inviscid flow at $Fr = 0.8$. Free surface profiles. Solid line: coupled finite volumes–BEM computation; o: BEM computation.

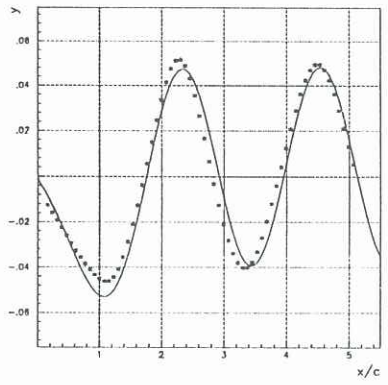

Figure 6: Salvesen profile at zero incidence. $Re = 3.5 \times 10^5$, $Fr = 0.591$. Free surface profiles. $*$: experimental data (Salvesen 1966). Solid line: viscous–inviscid computation.

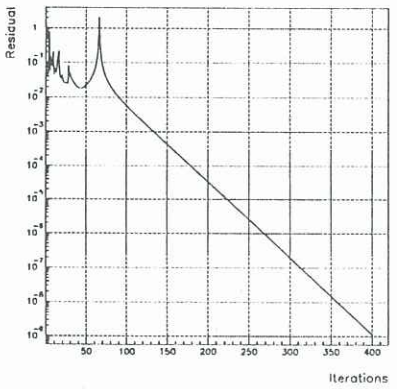

Figure 7: Salvesen profile at zero incidence. $Re = 3.5 \times 10^5$, $Fr = 0.591$. Convergence history of the $\tilde{\sigma}$ residual $\frac{|\tilde{\sigma}^{k+1} - \tilde{\sigma}^k|}{|\tilde{\sigma}^k|}$

ACKNOWLEDGEMENTS

The work was supported by the Italian Ministry of Merchant Marine in the frame of INSEAN research plan 1988-90.

REFERENCES

BALDWIN B., and LOMAX H., (1978), Thin-Layer Approximation and Algebric Model for Separated Turbulent Flows, AIAA paper, 78-257

DAWSON C. W.(1977), A Practical Computer Method for Solving Ship-Wave Problems, 2nd Int. Conf. on Numerical Ship Hydro., Berkeley.

DINH Q.H., GLOWINSKI R., PERIAUX J. and TERRASSON G. (1987), On the Coupling of Viscous and Inviscid Model for Incompressible Fluid Flows via Domain Decomposition, Proc. First Int. Symp. on Domain Decomposition Methods for P.D.E..

KWAK D., CHANG J.L.C., SHANKS S.P., CHAKRAVARTHY S.R. (1986), A Three-Dimensional Incompressible Navier–Stokes Flow Solver Using Primitive Variables, AIAA J., 23, 3, 390-396

LALLI F., CAMPANA E., BULGARELLI U. (1992), Numerical Simulation of Fully Nonlinear Steady Free Surface Flow, Int. Jou. Num. Methods in Fluids, 14, 1135–1149.

LOCK R.C. and WILLIAMS B.R. (1987), Viscous–Inviscid Interactions in External Aerodynamics, Prog. Aerospace Sci., 24, 51-171.

SALVESEN N.(1966), On Second Order Wave Theory for Submerged Two-Dimensional Bodies, 6th Sym. on Naval Hydro., Washington.